molecular pharmaceutics

Article

Cite This: *Mol. Pharmaceutics* XXXX, XXX, XXX−XXX

pubs.acs.org/molecularpharmaceutics

Antigen-Drug Conjugates as a Novel Therapeutic Class for the Treatment of Antigen-Specific Autoimmune Disorders

Chad J. Pickens,[†,§] Matthew A. Christopher,[†,§] Martin A. Leon,[‡] Melissa M. Pressnall,[†] Stephanie N. Johnson,[†] Sharadvi Thati,[†] Bradley P. Sullivan,[†] and Cory Berkland*[,†]

[†]Department of Pharmaceutical Chemistry, University of Kansas, 2095 Constant Avenue, Lawrence, Kansas 66047, United States

[‡]Department of Chemistry, University of Kansas, 1567 Irving Hill Road, Lawrence, Kansas 66045, United States

Supporting Information

ABSTRACT: Multiple sclerosis represents the world's most common cause of neurological disability in young people and is attributed to a loss of immune tolerance toward proteins of the myelin sheath. Typical treatment options for MS patients involve immunomodulatory drugs, which act nonspecifically, resulting in global immunosuppression. The study discussed herein aims to demonstrate the efficacy of antigen-specific immunotherapies involving the conjugation of disease causing autoantigen, $PLP_{139-151}$, and a potent immunosuppressant, dexamethasone. Antigen-drug conjugates (AgDCs) were formed using copper-catalyzed azide−alkyne cycloaddition chemistry with the inclusion of a hydrolyzable linker to maintain the activity of released dexamethasone. Subcutaneous administration of this antigen-drug conjugates to SJL mice induced with experimental autoimmune encephalomyelitis, protected the mice from a symptom onset throughout the 25 day study, demonstrating enhanced efficacy in comparison to dexamethasone treatment. These results highlight the benefits of co-delivery of autoantigens with immunosuppressant drugs as AgDCs for the treatment of autoimmune diseases.

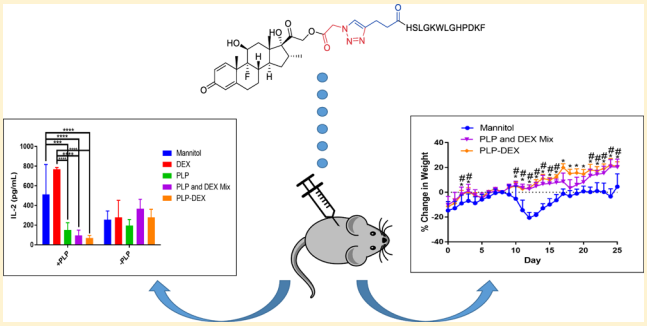

KEYWORDS: *autoimmunity, antigen-specific immunotherapy, copper-catalyzed azide−alkyne cycloaddition, experimental autoimmune encephalomyelitis, antigen-drug conjugate*

INTRODUCTION

The adaptive immune response is dependent on recognition of target antigens, and autoimmune diseases occur when the body fails to maintain tolerance toward self-antigens.[1] These self-antigens can be present in a number of host tissues in various organs, leading to many types of autoimmune diseases including multiple sclerosis (MS).[2] MS is the most common cause of neurological disability in young adults, affecting approximately 2.5 million patients worldwide,[3] and symptoms of the disease are highly variable.[4] While the mechanisms of disease induction have not been fully elucidated, a prevailing hypothesis is that the loss of immune tolerance toward proteins composing the myelin sheath, such as proteolipid protein (PLP) and myelin basic protein (MBP), triggers the recruitment of offending myelin-specific $CD4^+$ T cells, resulting in demyelination within the central nervous system (CNS).[5] Current therapies include monoclonal antibodies and corticosteroids; however, the treatment landscape for MS is expanding as our understanding of disease pathogenesis continues to evolve.[6] Corticosteroids have been a cornerstone for MS therapy, but the lack of specificity results in a wide range of side effects. Attempts have been made to develop antigen-specific immune therapies (ASITs) to reduce side effects and selectively retolerize the immune system to myelin sheath proteins. Despite being relatively safe, ASITs have yet to reduce the severity of MS.[7−9] Here, we present antigen-drug conjugates (AgDCs) as a combination of these approaches with the potential to boost the efficacy of ASIT while mitigating the detrimental side effects of current immunosuppressant therapies.

AgDCs merge two general approaches to combat autoimmunity: immunomodulatory agents and ASIT. ASIT provides the specificity necessary to reverse an immune response toward a particular antigen. ASIT has been effective for inducing tolerance toward allergens but has yet to emerge as an effective autoimmune therapy.[7−9] Immunomodulatory agents can effectively treat autoimmune diseases but suffer from systemic exposure and subsequent global immunosuppression, which can be problematic in immunocompromised patient populations by increasing its vulnerability to opportunistic infections. By chemically conjugating the antigen and immunomodulator, the antigen may target the immunomodulator to diseased cell populations, potentially limiting off-

Received: January 14, 2019
Revised: March 29, 2019
Accepted: April 30, 2019

DOI: 10.1021/acs.molpharmaceut.9b00063
Mol. Pharmaceutics XXXX, XXX, XXX−XXX

target side effects. The concept of AgDCs is similar to antibody-drug conjugates (ADCs); however, AgDCs likely achieve high affinity specificity by targeting endogenous autoantibodies or cognate B cell receptors, thus essentially flipping the mechanism of ADCs.

The design of AgDCs requires the selection of an appropriate antigen or epitope, an immune modulator, and a linking scheme. With this in mind, a murine experimental autoimmune encephalomyelitis (EAE) model exhibiting clinical and histopathological similarities to relapsing−remitting multiple sclerosis (RRMS) in humans[2] was selected to probe the proposed AgDC concept. The model is induced by administering an adjuvanted "vaccine" containing the antigenic epitope $PLP_{139-151}$. This particular EAE model is the $CD4^+$ T cell-mediated disease with B cell involvement, leading to primary demyelination of the axonal tracks in the CNS and subsequent progressive paralysis of the hind limbs.[10,11] Most importantly, this particular EAE model provided a simplified system for testing the efficacy of AgDCs wherein the disease may be induced with a specific peptide, $PLP_{139-151}$, and subsequently treated with an AgDC utilizing the same $PLP_{139-151}$ epitope.

Dexamethasone (DEX) was selected as the immune modulator for testing the AgDC concept. Our laboratory previously screened multiple immune modulators in combination with $PLP_{139-151}$ by using splenocytes derived from EAE mice.[12] DEX emerged as one of the most potent suppressors of proinflammatory cytokines when rechallenging EAE splenocytes with $PLP_{139-151}$ and also showed evidence of inducing markers of immune tolerance (e.g., upregulation of IL-10). DEX possesses the necessary potency required (pmol−nmol range)[13,14] because the dose typically used for the antigen-specific immunotherapy is on the order of milligrams of antigen per injection.[15] Finally, we rationalized that DEX must be released in order to escape the typical binding and internalization pathway associated with antigen recognition and processing. Thus, we designed an ester linker capable of releasing DEX from $PLP_{139-151}$ via hydrolysis with accelerated release under acidic conditions.

In this article, we outline the synthetic strategy, characterization, and biological screening of an AgDC containing $PLP_{139-151}$ and DEX. These two components were conjugated utilizing copper-catalyzed azide−alkyne cycloaddition (CuAAC) chemistry, and this linkage was characterized by HPLC and mass spectrometry. Additionally, AgDC linker stability was monitored over a short time frame to confirm the desired release of DEX. Finally, the efficacy of this AgDC was demonstrated first in vitro through the use of EAE splenocytes induced against $PLP_{139-151}$ and subsequently in vivo through subcutaneous administration to EAE mice.

MATERIALS AND METHODS

DEX, tris(3-hydroxypropyltriazolylmethyl)amine (THPTA), and sodium ascorbate (NaAsc) were purchased from Sigma-Aldrich (St. Louis, MO). Copper(II) sulfate pentahydrate ($CuSO_4{\cdot}5H_2O$) was purchased from Acros Organics (Geel, Belgium). 2,5-Dioxopyrrolidin-1-yl 2-azidoacetate, DBCO-PEG_4-maleimide, DBCO-NH_2, and MMAE-DBCO were purchased from Click Chemistry Tools, LLC (Scottsdale, AZ). Doxorubicin hydrochloride was purchased from LC Laboratories (Woburn, MA). Mertansine (DM1) was purchased from Carbosynth Limited (Berkshire, UK). All other chemicals and reagents were of analytical grade and were used as received without further purification.

The peptides $PLP_{139-151}$-Alk (*N*-terminal 4-pentynoic acid $PLP_{139-151}$) and $PLP_{139-151}$-N_3 (*N*-terminal 3-(2-(2-(2-azidoethoxy)ethoxy)ethoxy)-propanoic acid $PLP_{139-151}$) have been synthesized in our laboratory via solid- phase peptide synthesis on a Wang resin, but larger quantities of each peptide were obtained from Biomatik Corporation (Wilmington, DE). In each case, the linker 3-(2-(2-(2-azidoethoxy)ethoxy)-ethoxy)propanoic acid was purchased from PurePEG, LLC (San Diego, CA), and 4-pentynoic acid was purchased from Sigma-Aldrich (St. Louis, MO).

Synthesis of Azide-Functionalized DEX (DEX-N_3). DEX (842 μmol) was added to a flame-dried 250 mL round bottom flask with a stir bar and septa. Anhydrous MeCN (100 mL) was added under nitrogen then DIPEA (919 μmol, 1.09 eq.) via glass syringe. The flask was stirred for 10 min before azidoacetic acid NHS ester (908 μmol, 1.08 eq.) was added as a powder. The reaction mixture was stirred overnight at room temperature before being analyzed by HPLC. Additional equimolar aliquots of azidoacetic acid NHS ester were added, followed by stirring for 2 h at room temperature and analyzing by HPLC, until no additional benefit was observed. The crude reaction mixture was evaporated under a reduced pressure, then dissolved in 4:6 MeCN/H_2O, and purified by preparative HPLC. The resulting column fractions were evaporated under a reduced pressure to yield the final product as a white powder. ^{1}H NMR (500 MHz, DMSO-d_6, δ): 7.30 (d, J = 10.2 Hz, 1H), 6.23 (dd, J = 10.1, 1.9 Hz, 1H), 6.01 (t, J = 1.7 Hz, 1H), 5.45 (dd, J = 5.0, 1.4 Hz, 1H), 5.23 (s, 1H), 5.17 (d, J = 17.5 Hz, 1H), 4.90 (d, J = 17.6 Hz, 1H), 4.32−4.19 (m, 2H), 4.19−4.11 (m, 1H), 2.88 (dqd, J = 11.5, 7.2, 4.1 Hz, 1H), 2.62 (tdd, J = 13.6, 6.0, 1.7 Hz, 1H), 2.44−2.32 (m, 1H), 2.35−2.28 (m, 1H), 2.22−2.05 (m, 3H), 1.77 (dt, J = 11.2, 5.2 Hz, 1H), 1.70−1.58 (m, 1H), 1.56 (dd, J = 13.8, 2.0 Hz, 1H), 1.49 (s, 3H), 1.35 (qd, J = 12.9, 5.0 Hz, 1H), 1.08 (ddd, J = 12.1, 8.2, 4.1 Hz, 1H), 0.89 (s, 3H), 0.80 (d, J = 7.2 Hz, 3H). ^{13}C NMR (126 MHz, DMSO, δ): 204.36, 185.30, 168.28, 167.10, 152.77, 129.03, 124.12, 102.00, 100.61, 90.52, 70.63, 70.34, 69.00, 49.34, 48.09, 48.05, 47.87, 43.33, 35.69, 35.53, 33.67, 33.51, 31.92, 30.28, 27.32, 23.03, 22.98, 16.31, 15.15, 1.19. Expected $[M + H]^+$ = 476.2191 Da, observed $[M + H]^+$ = 476.2067 Da.

Synthesis of $PLP_{139-151}$-DEX. To a solution of $PLP_{139-151}$-Alk (93.6 μmol) in 120 mL of deionized H_2O was added DEX-N_3 (189.4 μmol, 2.02 eq.) in 12 mL of EtOH. A premixed solution (5.7 mL) of $CuSO_4{\cdot}5H_2O$ (38.1 μmol) and THPTA (189.8 μmol) in deionized H_2O was added to the reaction mixture, followed by 7.2 mL of NaAsc (726.9 μmol) in deionized H_2O. The reaction was allowed to stir at room temperature for 1 h before an aliquot was removed for analytical HPLC to monitor the reaction progress. After 3 h, the reaction mixture was concentrated under a reduced pressure and purified by preparative HPLC on a Waters XBridge BEH C_{18}, 5 μm, 130 Å stationary phase (19 × 250 mm) column using a gradient of MeCN in H_2O (constant 0.05% TFA). The isolated fractions were evaporated under a reduced pressure to remove residual MeCN, then frozen at −20 °C, and lyophilized to yield a white powder. Expected $[M + 2H]^{2+}$ = 1039.5224 Da, $[M + 3H]^{3+}$ = 693.3507 Da; observed $[M + 2H]^{2+}$ = 1039.5145 Da, $[M + 3H]^{3+}$ = 693.3478 Da.

Analytical Characterization. All HPLC chromatographic analyses were conducted on a Waters Alliance HPLC system

DOI: 10.1021/acs.molpharmaceut.9b00063
Mol. Pharmaceutics XXXX, XXX, XXX−XXX

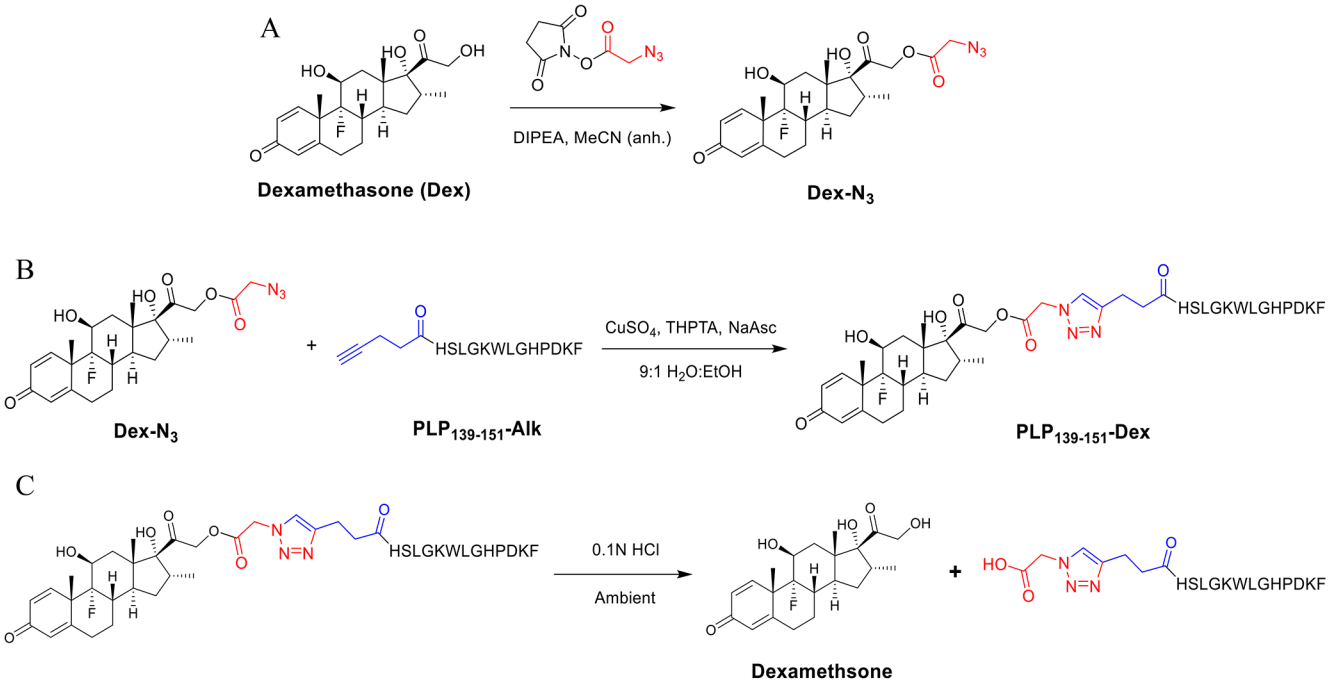

Figure 1. (A) Reaction scheme for the synthesis of DEX-N_3. (B) Reaction scheme for the synthesis of PLP-DEX. (C) Degradation of PLP-DEX to release parent drug, DEX.

equipped with either a diode array detector or dual wavelength UV−vis detector. For RP-HPLC, general chromatographic conditions employed a linear elution gradient from 5 to 95% acetonitrile in water (constant 0.05% trifluoroacetic acid) over 50 min, on a Waters XBridge BEH C_{18}, 3.5 μm, 130 Å stationary phase (4.6 × 150 mm), with a 1.0 mL/min flow rate and a 35 °C column temperature. For the semipreparative HPLC, a linear elution gradient of acetonitrile in water (constant 0.05% trifluoroacetic acid) over 20 min, on a Waters XBridge BEH C_{18}, 5 μm, 130 Å stationary phase (19 × 250 mm), with a 14.0 mL/min flow rate was used. Gradients were optimized for each run using the identical stationary phase in a 4.6 × 250 mm configuration.

LC−MS sample analysis was completed on a Waters Xevo G2, employing linear elution gradients of 15−100% acetonitrile in water (constant 0.1% formic acid) over 45 min, on a Waters XBridge BEH C_{18}, 1.7 μm, 130 Å stationary phase (0.075 × 250 mm), with a 0.5 μL/min flow rate and a 50 °C column temperature. Electrospray ionization, operating in the positive mode (ESI+), was used as the ionization source with a QTOF mass analyzer used for detection.

NMR spectra were collected on a Bruker Avance AVIII 500 MHz spectrometer equipped with a dual carbon/proton cryoprobe, and all samples were dissolved in 650 μL of D_2O or DMSO-d_6. Data processing was completed using MestReNova 11.0 (Santiago de Compostela, Spain).

Drug Release and Stability Studies. Release and stability studies were conducted via HPLC with UV detection by dissolving the compound of interest in various buffers (typically pH 7.0 phosphate, pH 5.5 acetate, deionized H_2O, etc.) and evaluating the release at temperatures and times relevant to the particular study. Peak integration is used for quantification, accounting for the initial purity of the PLP-DEX at $T = 0$.

Induction of EAE. In vitro and in vivo studies were performed through the use of 4−6 week old SJL/J (H-2) female mice purchased from Envigo Laboratories (Indianapolis, IN). All experiments were approved through the University's Institutional Animal Care and Use Committee with animal housing in pathogen-free conditions. An emulsion containing 200 μg of $PLP_{139-151}$ in complete Freund's adjuvant (CFA) was prepared by combining IFA and heat-killed *Mycobacterium tuberculosis* strain H37RA at a final concentration of 4 mg/mL with subsequent emulsification between CFA and PBS containing 200 μg of $PLP_{139-151}$. This PLP in CFA emulsion was administered to mice on day 0 via four subcutaneous injections of 50 μL each located above each shoulder and hind flank for a total of 0.2 mL. Additionally, intraperitoneal injections of pertussis toxin (100 ng in 100 μL of PBS) were administered on day 0 and day 2. Disease severity was recorded using the following clinical scoring system: 0, no clinical disease symptoms; 1, weakness or limpness of the tail; 2, weakness or partial paralysis of one or two hind limbs (paraparesis); 3, full paralysis of both hind limbs (paraplegia); 4, paraplegia plus weakness or paralysis of forelimbs; and 5, moribund (euthanasia necessary). Mouse body weight was also recorded daily throughout the duration of the studies.

In Vivo Efficacy in EAE Mice. In vivo studies were performed with nine mice per treatment group. Five mice were euthanized on day 14 (peak of disease), while the remaining mice were euthanized on day 25. Treatments were administered to mice through subcutaneous injection of 100 μL at the base of the neck on the back of the mouse on days 4, 7, and 10, following EAE induction. All treatments were dosed at a 200 nmol DEX basis in 40 mg/mL mannitol as the vehicle. Mice were weighed daily from day 0 and scored daily from day 7 until the end of the study at day 25.

Splenocyte Isolation. Spleens were harvested from EAE and healthy control mice on peak of disease or day 25 for in vitro and in vivo studies, respectively. Spleens were placed in 5 mL of RPMI 1640 containing L-glutamine and 1% penicillin−

DOI: 10.1021/acs.molpharmaceut.9b00063
Mol. Pharmaceutics XXXX, XXX, XXX−XXX

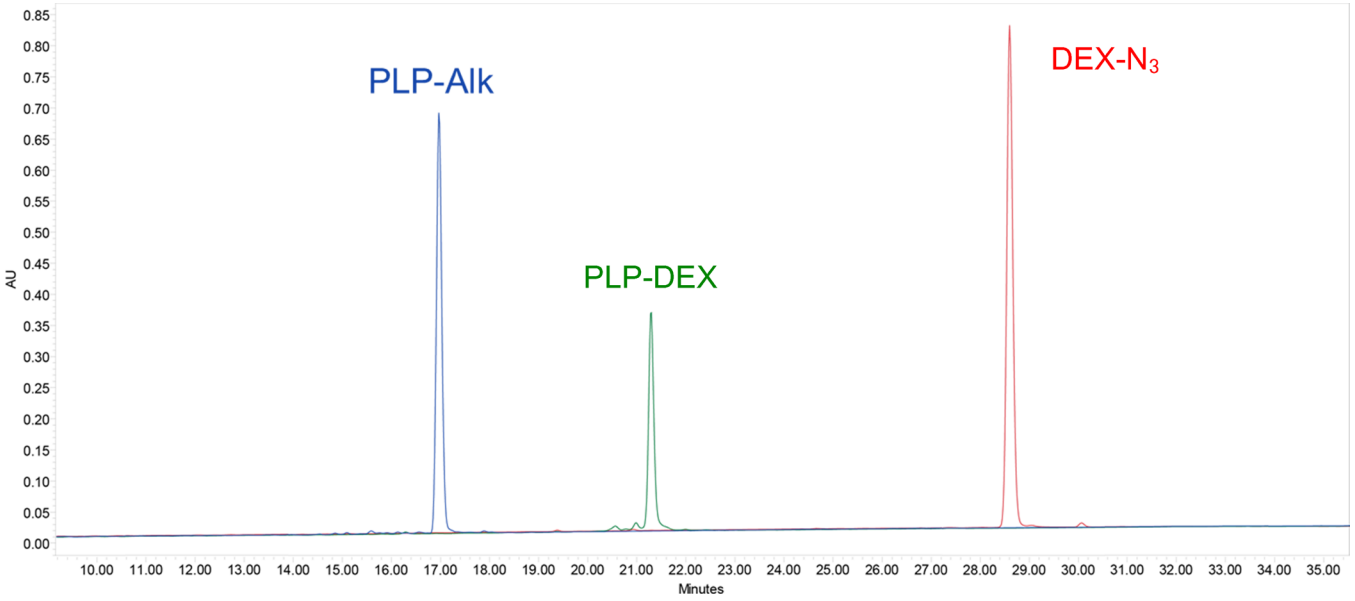

Figure 2. Representative analytical HPLC chromatogram showing the starting materials, PLP-Alk and DEX-N_3, along with the purified reaction product, PLP-DEX.

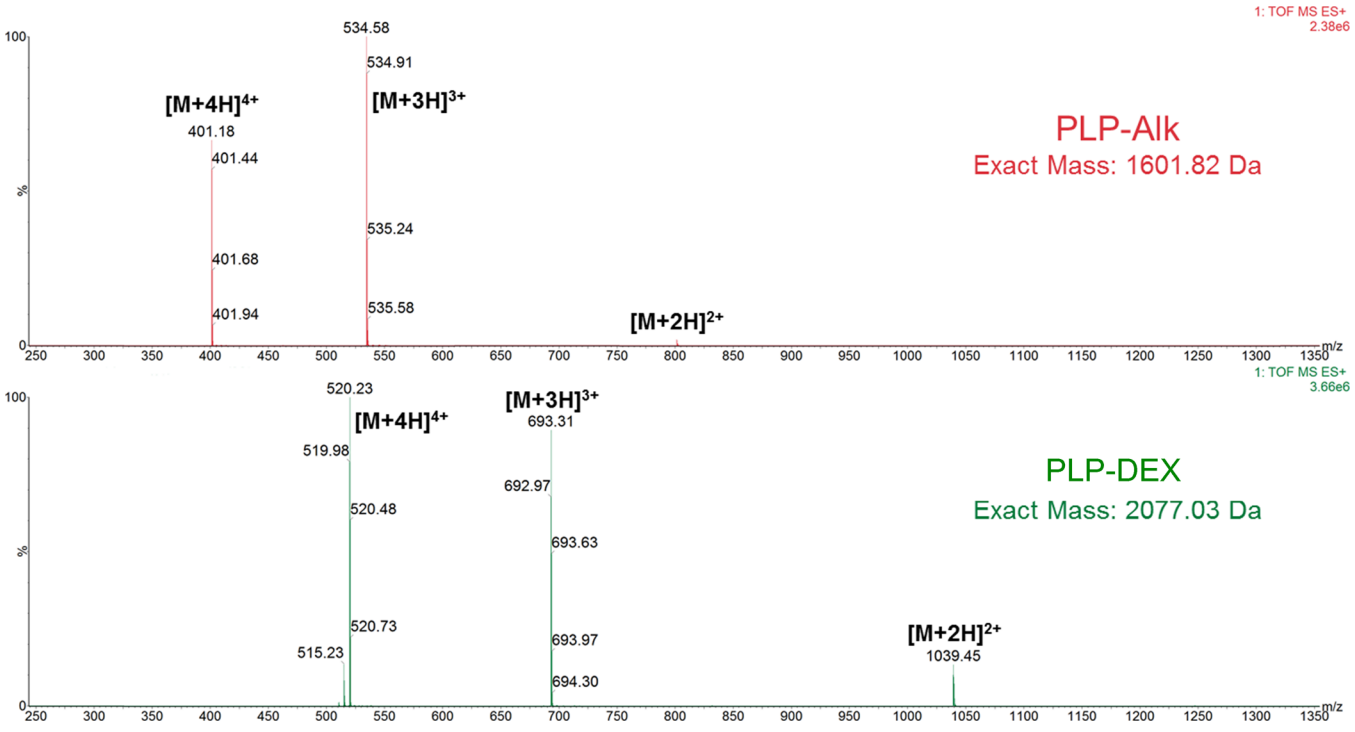

Figure 3. Representative mass spectral characterization showing multiple charge states of the starting peptide and the antigen-drug conjugate, PLP-DEX.

streptomycin and placed on ice for transportation. The spleens were pressed through sterile wire mesh with the use of a rubber 1 mL syringe plunger, and the cellular extract was collected and centrifuged at 1100 xg for 5 min. In order to lyse red blood cells, the cell pellet was resuspended in 5 mL of Gey's lysis solution for 5 min on ice. Quenching of the lysis solution was performed by adding 10 mL of RPMI 1640 supplemented with L-glutamine, 1% penicillin−streptomycin, and 10% fetal bovine serum (FBS) (complete RPMI, cRPMI). Cells were centrifuged at 1100 xg for 5 min and resuspended in cRPMI before counting in 0.04% trypan blue. Cultures with in vitro treatments or PLP rechallenge were kept at 37 °C and 5% CO_2.

Cell Metabolic Assay. Cellular metabolism was determined through the use of resazurin. Splenocytes were incubated with 75 μmol/L resazurin for 3 h. Change in fluorescence (ex 560/em 590) provides a measurement of metabolic reductive capacity. Results for in vitro treated samples were normalized against untreated controls, and background fluorescence was subtracted from all samples through fluorescence measurements on cRPMI containing

DOI: 10.1021/acs.molpharmaceut.9b00063
Mol. Pharmaceutics XXXX, XXX, XXX−XXX

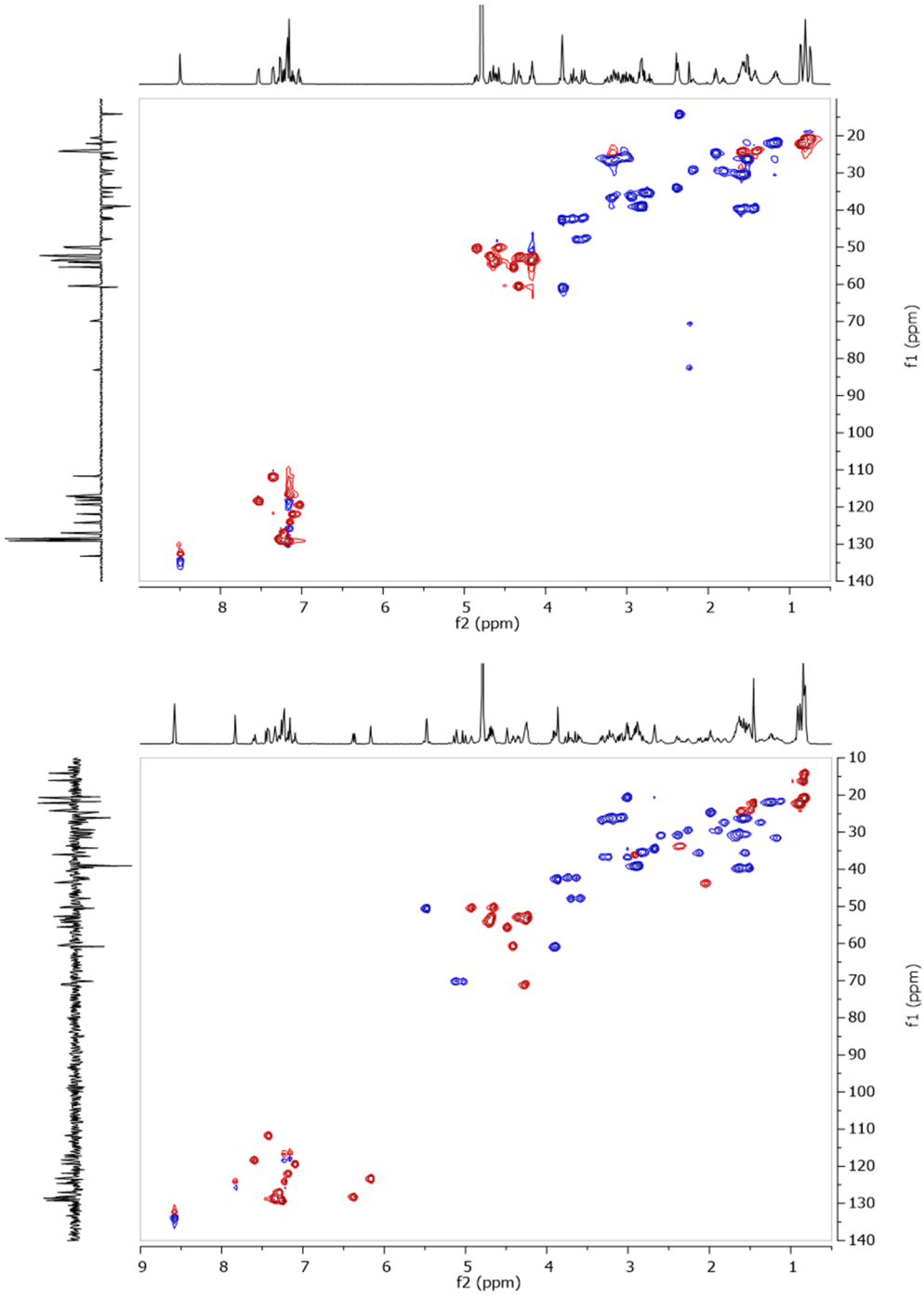

Figure 4. $^{1}H/^{13}C$ HSQC NMR data for $PLP_{139-151}$-Alk (top) and $PLP_{139-151}$-DEX (bottom).

resazurin. These readings were performed using a Spectramax M5 (molecular devices) plate reader.

Cytokine Response. Following the day 14 and day 25 splenocyte harvests from in vivo studies, in vitro splenocyte supernatants were collected after 96 h incubation with PLP. Incubation was performed at 1×10^6 cells/well in 96-well plates in the presence or absence of 25 μM PLP. The secretion of GM-CSF, IFN-γ, TNF-α, IL-2, IL-6, IL-10, IL-15, IL-17, IL-21, and IL-23 was measured using a U-Plex kit following the manufacturer instructions (Meso Scale Discovery).

Statistical Analysis. Statistical analysis of data was performed using two-way analysis of variance (ANOVA) and Tukey multiple comparison tests. IC_{50} studies were analyzed using a 4PL-sigmoidal function. Criteria for significance are as follows: $*p < 0.05$, $**p < 0.01$, $***p < 0.001$, $****p < 0.0001$. For Figure 7 and Figure 9 significant differences between the PLP and DEX mixture and mannitol vehicle control are denoted by $\#p < 0.05$. All statistical analyses were performed using GraphPad software (GraphPad Software Inc.).

RESULTS

Analytical Characterization of Chemical Entities. The constituent and conjugate molecules can be characterized by traditional chemical methods, including NMR, HPLC, LC–MS, and other spectroscopic means to confirm the structure of the entity. HPLC analysis of PLP-Dex with UV–vis detection

DOI: 10.1021/acs.molpharmaceut.9b00063
Mol. Pharmaceutics XXXX, XXX, XXX–XXX

provides typical purity values in excess of 93% following preparative HPLC purification (Figure 2). A similar analysis by LC−MS corroborates these results, showing a mass shift in the final conjugate indicative of attachment of DEX to PLP (Figure 3). From an NMR perspective, an added benefit to install the alkyne linker on PLP is the presence of a distinct resonance in $^{1}H/^{13}C$ heteronuclear single quantum coherence (HSQC) experiment, corresponding to the terminal alkyne correlation ($\delta(^{1}H) \approx 2.3$ ppm, $\delta(^{13}C) \approx 70$ ppm), which is present in a unique chemical environment and well separated from other signals (Figure 4 and Figure S1). After conjugation, this resonance undergoes a significant downfield shift ($\delta(^{1}H) \approx 7.8$ ppm) as it is incorporated as part of the conjugated triazole ring system (Figure 4). One additional advantage of conjugating hydrophobic drug molecules to hydrophilic peptides is the impact on aqueous solubility. The $PLP_{139-151}$ peptide is soluble in excess of 60 mg/mL, providing a significant enhancement in drug solubility in the resulting amphiphilic conjugates.

Conjugate Stability and Drug Release Kinetics. PLP-DEX contains an acid-labile ester linkage capable of releasing the unadulterated parent drug in acidic microenvironments present inside the cells. A study of the release kinetics (Figure 5) indicated that DEX is released over greater than 100 h in

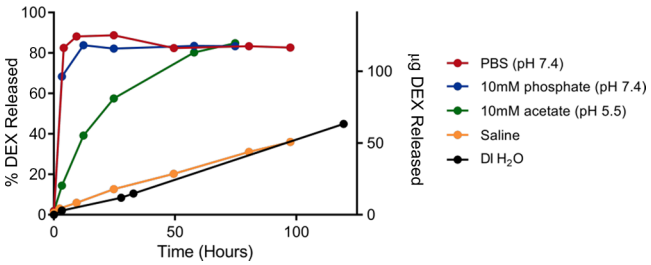

Figure 5. Release of DEX from $PLP_{139-151}$-DEX as a function of time and buffer, at 37 °C. Starting peptide concentration was 1 mg/mL, corrected for potency, and quantified via linear calibration curve.

unbuffered solutions and is released completely over approximately 50 h when in acidic conditions (pH 5.5). Interestingly, complete hydrolysis of the linker occurs in a few hours when in phosphate buffered solutions, indicating that phosphate anions catalyze the release of DEX from PLP, likely through the nucleophilic attack on the ester bond. Due to this finding, in vivo administration of PLP-DEX was carried out in 40 mg/mL mannitol to prevent hydrolysis before injection.

IC_{50} Determination of Conjugates and Payload. In order to determine the impact of the CuAAC chemical linkage on the activity of esterified DEX, EAE splenocytes harvested at peak of disease (day 12) were isolated and treated with DEX or PLP-DEX over a range of concentrations. After 120 h, a resazurin assay was performed to assess cellular metabolism, and these data were normalized to untreated EAE splenocytes (Figure 6). These data provide calculated IC_{50} values for DEX and PLP-DEX of 6.84 ± 4.18 and 7.55 ± 2.80 nM, respectively. This result indicates that DEX maintains the activity after the release from the AgDC and demonstrates the rapid release of DEX from the acid-labile ester linkage in an in vitro setting, as evidenced by the similar IC_{50} values obtained for the free drug and the AgDC.

In Vivo Screening of Conjugates. In vivo efficacy of PLP-DEX in the treatment of EAE was determined through

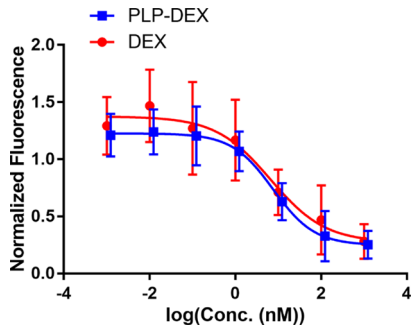

Figure 6. Resorufin fluorescence of EAE splenocytes treated with free DEX or PLP-DEX for 120 h (n = 6). These data are normalized to untreated EAE splenocytes. Calculated IC_{50} values for these treatments are 6.84 ± 4.18 and 7.55 ± 2.80 nM for DEX and PLP-DEX, respectively. Reported values are with standard error.

subcutaneous administration of the conjugate and component treatments at a dose equivalent to 200 nmol DEX. Treatments were administered in 40 mg/mL mannitol on days 4, 7, and 10 with n = 9 before day 14 and n = 4 after day 14. Five mice in each treatment group were chosen at random and euthanized at peak of disease in order to assess splenocyte response to 25 μM PLP rechallenge. This in vivo schedule allows for the determination of the effectiveness of AgDCs in ameliorating EAE clinical symptoms and mechanistic insight into changes in cellular expression after treatment.

In vivo clinical score data indicate the importance of conjugation of DEX to the antigen of interest (Figures 7). EAE mice treated with the AgDC demonstrated no clinical symptoms throughout the 25 day study (Figure 7B and 8). This represents a vast improvement over the free drug, DEX (Figure 7A), which appears to have no clinical effect on the EAE model at a 200 nmol dose. Similar to the AgDC, administration of a combination of the components, PLP and DEX, ameliorates symptoms and appears to delay the onset of paralysis in EAE mice (Figure 7B); however, this coadministration is less effective than co-delivery through direct conjugation. Additionally, coadministration of PLP and DEX as a mixture resulted in delayed symptom onset in the mice that developed the disease (Table 1). Treatment with individual components, PLP or DEX, had no significant effect on reducing EAE symptoms (Figure 7A). Similar trends are observed in animal weight data (Figure 9), in which weight gain is associated with a healthy mouse and weight loss correlates to symptom severity. In combination therapies (Figure 9B), continuous weight gain is observed throughout the duration of the study. Conversely, mice treated with individual components and mannitol (Figure 9A) displayed a significant weight loss leading up to disease remission.

As previously stated, five mice were euthanized on day 14 in order to assess cellular differences due to the various in vivo treatments (Figure 10 and Figures S2−S8). Of note, at day 14 a small but significant reduction in GM-CSF (Figure 10A), an inflammatory cytokine, was observed for combination therapies. Additionally, detection of IL-2 (Figure 10B), a cytokine associated with T-cell proliferation, was greatly diminished in combination therapies and the PLP control. These results demonstrate the early immunosuppressive effects of combination treatments containing DEX. Comparisons of GM-CSF and IL-2 between the mixture of PLP and DEX and the AgDC revealed no significant differences between coadministration and co-delivery at this stage of treatment.

DOI: 10.1021/acs.molpharmaceut.9b00063
Mol. Pharmaceutics XXXX, XXX, XXX−XXX

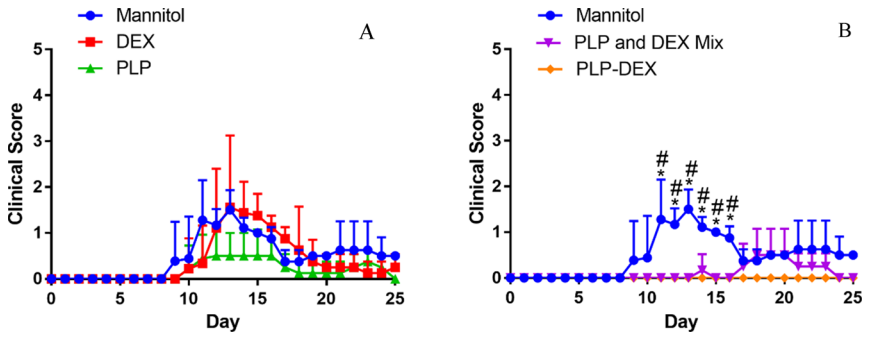

Figure 7. Clinical score data for EAE mice treated in vivo with (A) free DEX and free $PLP_{139-151}$ and (B) a mixture of free DEX and $PLP_{139-151}$ and the PLP-DEX conjugate. Treatments were administered subcutaneously on days 4, 7, and 10 at doses of 200 nmol DEX basis. $N = 9$ until day 14 and $n = 4$ after day 14. Five mice were chosen at random from each group on day 14 for euthanasia in order to assess splenocyte differences in treatment groups around peak of disease. Data provided is mean ± SD. *$p < 0.05$ for mannitol vs PLP-DEX and #$p < 0.05$ for mannitol vs PLP and DEX mix.

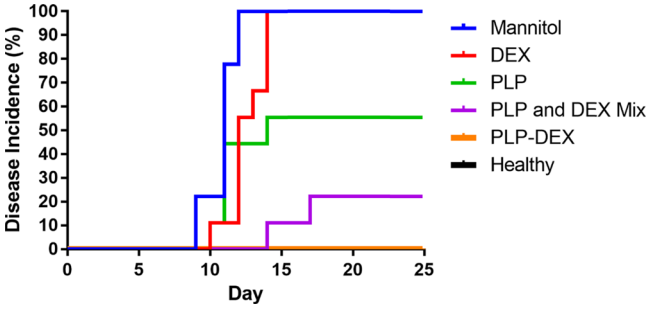

Figure 8. Percent disease incidence for all treatment groups where disease onset is characterized by a clinical score ≥ 1. $N = 9$ until day 14 and $n = 4$ after day 14. Five mice were chosen at random from each group on day 14 for euthanasia in order to assess splenocyte differences in treatment groups around peak of disease.

One notable difference between these treatment groups in cytokine expression was observed in IL-10 (Figure 10C), in which the mixture treatment group experienced a significant reduction in IL-10 expression compared to control. This result was not observed in the conjugate treatment group and may account for the differences in efficacy observed in vivo by maintaining an anti-inflammatory effector cell population. Numerous other cytokines were analyzed; however, no significant changes associated with treatment efficacy were observed in the expression of these cytokines (Figures S2–S8).

DISCUSSION

Clinical researchers attempting to treat autoimmune diseases such as MS have historically focused on either administering drugs to suppress and/or modulate the immune response (e.g., classic immunosuppression) or more recently, ASIT (e.g., long treatment regimens of low doses of antigen or altered antigen analogs).[16] Currently, potent immunomodulatory drugs represent the core treatment options for MS patients, but these drugs act in a nonspecific manner and may eliminate or suppress healthy immune cell populations. Conversely, although ASIT is relatively safe, this approach has not yielded sufficient efficacy to suppress autoimmunity.[7−9] Through direct conjugation of potent immunomodulators to self-antigens, targeted immunosuppression of self-reactive populations may boost the efficacy of ASIT and diminish the side effects associated with immunosuppressants.

The encephalitogenic peptide selected as the targeting moiety is a portion of the intracellular loop[17] of the full-length transmembrane protein, $PLP_{139-151}$. Previous studies have shown the impact of $PLP_{139-151}$ sequence variability on TCR binding affinity,[18] highlighting the influence of side chain interactions in the major histocompatibility class II binding pocket. Therefore, disrupting interactions through traditional synthetic methods targeting side chain residues of the native sequence were hypothesized to alter conjugate binding and/or uptake. To circumvent these potential deleterious effects, all modifications to the targeting antigen occurred through the *N*-terminal amino acid and were installed via heterobifunctional linkers as the final step of solid-phase peptide synthesis before cleavage from the resin. Linker length, flexibility, and stability were key AgDC design considerations. The overarching strategy utilizing CuAAC chemistry enabled rapid and efficient synthesis of PLP-DEX (Figure 1) and related conjugates.

Data reported here support a growing base of literature highlighting the benefits of delivering autoantigen alongside immunomodulators. Although historically categorized as an immunosuppressant, DEX is now known to skew cellular responses toward immune tolerance via multiple mechanisms.[19−22] For example, DEX was shown to enhance CTLA-4 expression during T cell activation, thus countering the typical B7/CD28 proinflammatory costimulatory signal.[22] DEX also inhibited IL-12 secretion by dendritic cells and increased FoxP3 expression in naïve T lymphocyte cocultures.[20] DEX was reported to induce expression of indoleamine 2,3-dioxygenase (IDO), an enzyme implicated in T cell tolerance[21] that has been used to create "tolerogenic dendritic

Table 1. Disease Incidence Rate and Mean Day of Disease Onset ± SD for each Treatment Group[a]

parameter	mannitol	DEX	PLP	PLP and DEX mix	PLP-Dex
incidence rate (fraction)	9/9	9/9	5/9	2/9	0/9
mean day of onset ± SD	10.8 ± 1.1	12.6 ± 1.3	11.4 ± 1.5	15.5 ± 2.1	

[a]Incidence rate is represented as a fraction of total mice per treatment group with a clinical score ≥ 1. Mean day of onset is calculated only for symptomatic animals.

DOI: 10.1021/acs.molpharmaceut.9b00063
Mol. Pharmaceutics XXXX, XXX, XXX−XXX

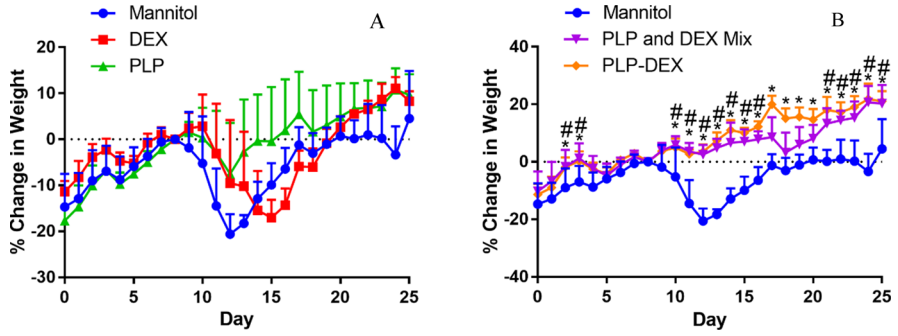

Figure 9. Mouse weight data for EAE mice treated in vivo with (A) free DEX and free $PLP_{139-151}$ and (B) a mixture of free DEX and $PLP_{139-151}$ and the PLP-DEX conjugate. Data are normalized to the individual mouse weight at day 8 (symptom onset). Treatments were administered subcutaneously on days 4, 7, and 10 at doses of 200 nmol DEX basis. $N = 9$ until day 14 and $n = 4$ after day 14. Five mice were chosen at random from each group on day 14 for euthanasia in order to assess splenocyte differences in treatment groups around peak of disease. *$p < 0.05$ for mannitol vs PLP-DEX and #$p < 0.05$ for mannitol vs PLP and DEX mix.

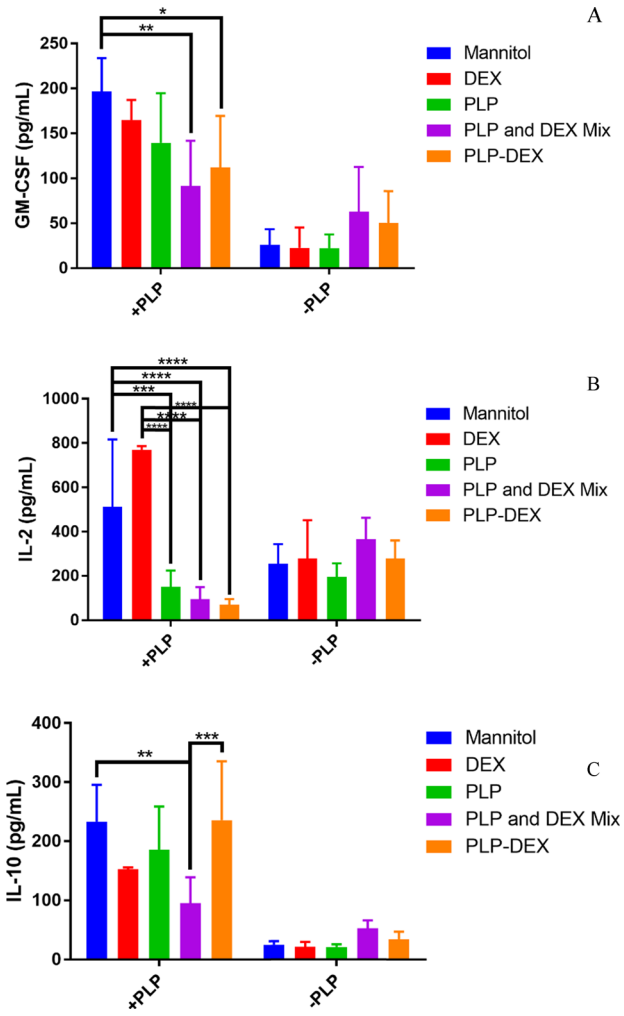

Figure 10. Levels of (A) GM-CSF, (B) IL-2, and (C) IL-10 were observed at peak of disease (day 14) after isolated splenocytes from in vivo treated mice were incubated for 96 h with 25 μM PLP. $N = 5$, *$p < 0.05$, **$p < 0.01$, ***$p < 0.001$, ****$p < 0.0001$.

cells" (defined as high TLR-2, CXCR4, and CCR7 expression levels) from healthy donors.[19]

Because of these pluripotent mechanisms, some have tested DEX as an adjuvant that can be coadministered along with antigen as a means to induce antigen-specific immune tolerance.[20,23,24] Previously, Kang and colleagues demonstrated the desensitization specific to $OVA_{323-339}$ peptide after coadministration of this peptide alongside DEX.[25] Additionally, applying this strategy of coadministration to the NOD autoimmune diabetes model protected nearly all mice from a disease induction throughout the study period, suggesting these therapies may be adapted for application to numerous autoimmune diseases with known autoantigens.[25] Further development of this treatment strategy by Peine et al. utilized acetalated dextran particles as a co-delivery vehicle for a myelin oligodendrocyte glycoprotein (MOG) peptide and DEX in EAE, and administration of these microparticles to EAE mice after the disease onset resulted in the significant reduction in disease severity when both components were present.[26] With such striking differences in vivo between combination therapies and free DEX, our findings highlight the advantages associated with the delivery of an immunosuppressive drug in the context of the autoantigens of interest. Furthermore, conjugation of DEX to $PLP_{139-151}$ may maximize the co-delivery of autoantigen and immunomodulator in larger organisms, enhancing drug potency as demonstrated and potentially limiting off-target effects.

CONCLUSIONS

Antigen-drug conjugates represent a novel class of therapeutics with broad applicability to a variety of antigen-specific autoimmune disorders. By combining the benefits of two traditional treatment approaches, ASIT and immunomodulatory therapy, AgDCs employ a synergistic approach by conjugating the antigen to the immunomodulatory agent. The enhanced specificity associated with therapeutics of this class may help to minimize global immunosuppression often observed with immunomodulatory small-molecule treatments. This publication serves as an introduction to the modular synthetic design achieved in our laboratory and demonstrates both efficacy and safety of in vivo AgDC treatment in a mouse model of MS in which the autoreactive antigen is identified. The EAE model provides a valuable system for the initial testing of AgDCs as induction and treatment of the disease can be achieved utilizing a single antigen epitope, in this case, $PLP_{139-151}$. Subcutaneous treatment with free DEX at a 200 nmol dose appears to have little effect compared to control on modifying the disease course. EAE mice treated in vivo with PLP-DEX; however, demonstrated no onset of disease over a 25 day period and appeared healthy throughout the study, which demonstrates the efficacy achievable with co-delivery of

DOI: 10.1021/acs.molpharmaceut.9b00063
Mol. Pharmaceutics XXXX, XXX, XXX−XXX

the antigen and immunomodulator. The modular fashion of this AgDC approach, coupled with the consistency and specificity of the chemistries employed, makes AgDCs a potential disease-specific therapeutic class for autoimmune disorders.

■ ASSOCIATED CONTENT

Supporting Information

The Supporting Information is available free of charge on the ACS Publications website at DOI: 10.1021/acs.molpharmaceut.9b00063.

HSQC NMR data for DEX-N_3; levels of IFN-γ at peak of disease; levels of IL-6 at peak of disease; levels of IL-15 at peak of disease; levels of IL-17A at peak of disease; levels of IL-21 at peak of disease; levels of IL-23 at peak of disease; and levels of TNF-α at peak of disease (PDF)

■ AUTHOR INFORMATION

Corresponding Author

*E-mail: berkland@ku.edu. Phone: (785) 864-1455. Fax: (785) 864-1454.

ORCID

Matthew A. Christopher: 0000-0002-5008-8771

Cory Berkland: 0000-0002-9346-938X

Author Contributions

§C.J.P. and M.A.C. contributed equally to this work.

Notes

The authors declare no competing financial interest.

■ ACKNOWLEDGMENTS

We gratefully acknowledge the support from the National Institutes of Health Graduate Training Program in Dynamic Aspects of Chemical Biology grant (T32 GM008545) from the National Institutes of General Medical Sciences (C.J.P., M.A.L., and S.N.J.), and the Howard Rytting predoctoral fellowship from the Department of Pharmaceutical Chemistry at the University of Kansas (C.J.P.). Additionally, we would like to acknowledge the support from the National Institutes of Health Biotechnology Training grant (NIH0073415) (M.A.C.). We would also like to thank the KU NMR facility and the KU Macromolecule and Vaccine Stabilization Center (MVSC) for collaboration and instrument use. Also, support for the NMR instrumentation was provided by NIH Shared Instrumentation grant no. S10RR024664 and NSF Major Research Instrumentation award no. 1625923. We also thank Tom Prisinzano for the useful discussions on synthetic strategy.

■ REFERENCES

(1) Murphy, K. M. *Janeway's Immunobiology*. 8th ed.; Garland Science: New Tork, 2012.

(2) Perl, A. *Autoimmunity Methods and Protocols*. 2 nd ed.; Humana Press, 2012.

(3) Compston, A..; Coles, A. Multiple Sclerosis. *Lancet* **2002**, *359*, 1221−1231.

(4) Dendrou, C. A.; Fugger, L.; Friese, M. A. Immunopathology of multiple sclerosis. *Nat. Rev. Immunol* **2015**, *15*, 545−58.

(5) Podbielska, M.; Banik, N.; Kurowska, E.; Hogan, E. Myelin recovery in multiple sclerosis: the challenge of remyelination. *Brain Sci.* **2013**, *3*, 1282−1324.

(6) Karussis, D. Immunotherapy of multiple sclerosis: the state of the art. *BioDrugs* **2013**, *27*, 113−148.

(7) Bielekova, B.; Goodwin, B.; Richert, N.; Cortese, I.; Kondo, T.; Afshar, G.; Gran, B.; Eaton, J.; Antel, J.; Frank, J. A.; McFarland, H. F.; Martin, R. Encephalitogenic potential of the myelin basic protein peptide (amino acids 83−99) in multiple sclerosis: Results of a phase II clinical trial with an altered peptide ligand. *Nat. Med.* **2000**, *6*, 1167.

(8) Kappos, L.; Comi, G.; Panitch, H.; Oger, J.; Antel, J.; Conlon, P.; Steinman, L.; Comi, G.; Kappos, L.; Oger, J.; Panitch, H.; Rae-Grant, A.; Castaldo, J.; Eckert, N.; Guarnaccia, J. B.; Mills, P.; Johnson, G.; Calabresi, P. A.; Pozzilli, C.; Bastianello, S.; Giugni, E.; Witjas, T.; Cozzone, P.; Pelletier, J.; Pöhlau, D.; Przuntek, H.; Hoffmann, V.; Bever, C., Jr; Katz, E.; Clanet, M.; Berry, I.; Brassat, D.; Brunet, I.; Edan, G.; Duquette, P.; Radue, E.-W.; Schött, D.; Lienert, C.; Taksaoui, A.; Rodegher, M.; Filippi, M.; Evans, A.; Bourgouin, P.; Zijdenbos, A.; Salem, S.; Ling, N.; Alleva, D.; Johnson, E.; Gaur, A.; Crowe, P.; Liu, X.-J. Induction of a non-encephalitogenic type 2 T helper-cell autoimmune response in multiple sclerosis after administration of an altered peptide ligand in a placebo-controlled, randomized phase II trial. *Nat. Med.* **2000**, *6*, 1176.

(9) Freedman, M. S.; Bar-Or, A.; Oger, J.; Traboulsee, A.; Patry, D.; Young, C.; Olsson, T.; Li, D.; Hartung, H.-P.; Krantz, M.; Ferenczi, L.; Verco, T. A phase III study evaluating the efficacy and safety of MBP8298 in secondary progressive MS. *Neurology* **2011**, *77*, 1551−1560.

(10) Miller, S. D.; Karpus, W. J. Experimental autoimmune encephalomyelitis in the mouse. *Curr. Protoc. Immunol.* **2010**, *15*, 1.

(11) Miyagaki, T.; Fujimoto, M.; Sato, S. Regulatory B cells in human inflammatory and autoimmune diseases: from mouse models to clinical research. *Int. Immunol.* **2015**, *27*, 495−504.

(12) Northrup, L.; Sullivan, B. P.; Hartwell, B. L.; Garza, A.; Berkland, C. Screening Immunomodulators To Skew the Antigen-Specific Autoimmune Response. *Mol. Pharmaceutics* **2017**, *14*, 66−80.

(13) Brandl, C.; Haas, C.; d'Argouges, S.; Fisch, T.; Kufer, P.; Brischwein, K.; Prang, N.; Bargou, R.; Suzich, J.; Baeuerle, P. A.; Hofmeister, R. The effect of dexamethasone on polyclonal T cell activation and redirected target cell lysis as induced by a CD19/CD3-bispecific single-chain antibody construct. *Cancer immunol. Immunother* **2007**, *56*, 1551−63.

(14) Palma, L.; Sfara, C.; Antonelli, A.; Magnani, M. Dexamethasone restrains ongoing expression of interleukin-23p19 in peripheral blood-derived human macrophages. *BMC pharmacol.* **2011**, *11*, 8.

(15) Peakman, M.; Dayan, C. M. Antigen-specific immunotherapy for autoimmune disease: fighting fire with fire? *Immunol.* **2001**, *104*, 361−6.

(16) Cox, L.; Compalati, E.; Kundig, T.; Larche, M. New directions in immunotherapy. *Curr. allergy asthma rep.* **2013**, *13*, 178−95.

(17) Greer, J. M. Autoimmune T-cell reactivity to myelin proteolipids and glycolipids in multiple sclerosis. *Mult Scler Int* **2013**, *2013*, 151427.

(18) Kuchroo, V. K.; Greer, J. M.; Kaul, D.; Ishioka, G.; Franco, A.; Sette, A.; Sobel, R. A.; Lees, M. B. A single TCR antagonist peptide inhibits experimental allergic encephalomyelitis mediated by a diverse T cell repertoire. *J. Immunol.* **1994**, *153*, 3326−3336.

(19) García-González, P.; Morales, R.; Hoyos, L.; Maggi, J.; Campos, J.; Pesce, B.; Gárate, D.; Larrondo, M.; González, R.; Soto, L.; Ramos, V.; Tobar, P.; Molina, M. C.; Pino-Lagos, K.; Catalán, D.; Aguillón, J. C. A short protocol using dexamethasone and monophosphoryl lipid A generates tolerogenic dendritic cells that display a potent migratory capacity to lymphoid chemokines. *J. trans med.* **2013**, *11*, 128.

(20) Gong, Y. B.; Huang, Y. F.; Li, Y.; Han, G. C.; Li, Y. R.; Wang, D. J.; Du, G. P.; Yu, J. F.; Song, J. Experimental study of the mechanism of tolerance induction in dexamethasone-treated dendritic cells. *Med sci monit.* **2011**, *17*, BR125−BR131.

(21) Grohmann, U.; Volpi, C.; Fallarino, F.; Bozza, S.; Bianchi, R.; Vacca, C.; Orabona, C.; Belladonna, M. L.; Ayroldi, E.; Nocentini, G.; Boon, L.; Bistoni, F.; Fioretti, M. C.; Romani, L.; Riccardi, C.; Puccetti, P. Reverse signaling through GITR ligand enables dexamethasone to activate IDO in allergy. *Nat. Med.* **2007**, *13*, 579−586.

DOI: 10.1021/acs.molpharmaceut.9b00063
Mol. Pharmaceutics XXXX, XXX, XXX−XXX

(22) Xia, M.; Gasser, J.; Feige, U. Dexamethasone enhances CTLA-4 expression during T cell activation. *Cell. Mol. Life Sci.* **1999**, *55*, 1649−1656.
(23) Zheng, G.; Zhong, S.; Geng, Y.; Munirathinam, G.; Cha, I.; Reardon, C.; Getz, G. S.; van Rooijen, N.; Kang, Y.; Wang, B.; Chen, A. Dexamethasone promotes tolerance in vivo by enriching $CD11c^{lo}$ $CD40^{lo}$ tolerogenic macrophages. *Eur. J. Immunol.* **2013**, *43*, 219−227.
(24) Unger, W. W. J.; Laban, S.; Kleijwegt, F. S.; van der Slik, A. R.; Roep, B. O. Induction of Treg by monocyte-derived DC modulated by vitamin D_3 or dexamethasone: differential role for PD-L1. *Eur. J. Immunol.* **2009**, *39*, 3147−59.
(25) Kang, Y.; Xu, L.; Wang, B.; Chen, A.; Zheng, G. Cutting Edge: Immunosuppressant as Adjuvant for Tolerogenic Immunization. *J. Immunol* **2008**, *180*, 5172−5176.
(26) Peine, K. J.; Guerau-de-Arellano, M.; Lee, P.; Kanthamneni, N.; Severin, M.; Probst, G. D.; Peng, H.; Yang, Y.; Vangundy, Z.; Papenfuss, T. L.; Lovett-Racke, A. E.; Bachelder, E. M.; Ainslie, K. M. Treatment of Experimental Autoimmune Encephalomyelitis by Codelivery of Disease Associated Peptide and Dexamethasone in Acetalated Dextran Microparticles. *Mol. Pharmaceutics* **2014**, *11*, 828−835.

DOI: 10.1021/acs.molpharmaceut.9b00063
Mol. Pharmaceutics XXXX, XXX, XXX−XXX